

A countermeasure to improve outage performance of interference-limited microwave radio links

Contre-mesure pour améliorer les performances à une mise hors-service d'une liaison micro-ondes à interférence limitée.

Mohsen Kavehrad, *University of Ottawa, Department of Electrical Engineering, Ottawa, Ontario K1N 6N5.*

In this paper a hybrid radio architecture is proposed. A performance model is presented. The associated outage performance is evaluated for a hybrid radio route which consists of a number of digital point-to-point microwave radio channels with a parallel atmospheric optical link protecting all of them against frequency-selective fading and RF interference. Our numerical results show an acceptable performance can be achieved.

Cet article propose une architecture radio-hybride et on y présente un modèle pour en établir la performance. On y étudie notamment la performance à la mise hors-service d'une liaison radio-hybride composée d'un certain nombre de canaux-radio micro-ondes en ligne directe et d'un lien optique atmosphérique en parallèle servant à les protéger contre l'affaiblissement sélectif et l'interférence radio-fréquence (RF). Les résultats numériques obtenus montrent qu'une performance acceptable peut être obtenue.

Introduction

Some digital radio routes, especially those at junction stations, are presently limited in performance by severe RF interference (RFI) from other existing digital as well as analog radios. An atmospheric optical line-of-sight communications link is immune to such an interference. In this work, we propose a hybrid radio diversity architecture and we develop a simple performance model that, to a first order, approximates the outage performance of the system. In this architecture an atmospheric optical channel provides diversity for the radio link against both interference and multipath fading.

To obtain an approximate performance assessment model, we rely on B. King's observation¹ that the dispersive fading of a terrestrial radio link is a clear-weather phenomenon, while weather-related optical outages occur mostly during unclear weather conditions such as in fog, heavy rain, etc. This observation is not completely true, because sometimes fog occurs during the same meteorological conditions that cause frequency-selective multipath fading.² This condition occurs when temperature inversions associated with multipath fading tend to trap fog in the lower levels of the atmosphere. Fog, of course, can cause outage of the optical link. There could also be other kinds of optical link outages, e.g., an outage due to a thick smoke that may very well occur while the radio link is subject to dispersive fading. Hence, the matter requires further research. Nevertheless, in this preliminary work we assume all the optical outages occur during times that the radio link is not subject to dispersive (frequency-selective) fading. However, RF interference is assumed to be present at all times.

During such times, it is assumed that the radio channel is subject to small-variance flat fades. Such scintillations are characterized by a log-normal probability density function.³ There are also fades with a larger flat component and a shallow-notch superimposed on the flat part. It is hoped that a log-normal density function describes such fading amplitude on the microwave channel. Measured data⁴ show that the standard deviation of the fading amplitude density function covering both types of fades may range to 7 dB. In addition, the radio link is subject to RF interference, as stated

earlier. The signal-to-interference (amplitude) ratio follows a log-normal density with a 60 dB mean and a standard deviation of 4 dB for about 20 per cent of the radio channels in the 4 GHz frequency band.⁴

The intensity of an optical beam propagating through a turbulent atmosphere has been characterized by a random variable whose logarithm follows a Gaussian probability density function with a standard deviation that in decibels will extend to 25 dB in strong turbulence.⁵ We take this density function as a conditional density, conditioned upon a known fading status for the radio link. By making this assumption, the mathematical issue of negative correlation between having the dispersive fades on the radio link and having an unfaded optical signal at the same time can be set aside and the microwave and optical channel signals may then be treated as independent processes.

In the absence of a deep microwave frequency-selective fade notch, a simple selection diversity power combiner operating in the IF or RF range can compare the received signal power levels on the two channels and select the stronger. Mathematically, this selection process is equivalent to choosing the maximum of the two signal-to-total noise ratio (SNR) values that depend on the log-normal fading parameters on the two channels. Having determined the density of the signal-to-total noise ratio at the combiner output, we may determine the outage value by integrating the density function over the range of output signal-to-noise ratio values for which an unacceptable error probability performance results.

In practice, microwave radio signals are relayed over several radio hops. If an optical channel is used to provide diversity and protect the radio signals against interference, we have to trace the interference to its source and build an atmospheric optical route in parallel to the radio route that is interfered by RFI, starting with the interference-free signal transmitted on the route.

In the next section, we propose an architecture for sending frequency-division-multiplexed 90 Mbps/64-QAM IF signals over an optical channel as a diversity back-up for the radio signals. We

also present an overview on optical propagation and overall system design. In the third section, we analyze the performance of such a hybrid radio. We will then present our conclusions.

Proposed hybrid architecture

A block diagram of the proposed architecture is depicted in Figure 1. Twelve IF channels (90 Mbps/64-QAM) signals are frequency-division-multiplexed in the MHz range. The outcome intensity modulates a laser light beam. The light transmitted by a telescope is received by a larger telescope. The collected light is focused over the active surface of a photodiode. The photo-detected signal, after amplification, is applied to a bank of band-pass filters that separate the IF 90 Mbps signals. Similar signals, received over the radio route, are diversity combined with the ones from the optical channel and the outcomes are delivered to the 90 Mbps/64-QAM receivers. In this paper, we assume the multiplexed signals intensity modulate a laser beam without causing its operating point to drift into the laser nonlinear operation regime. Therefore, intermodulation distortion will not be considered. The optical channel may interface the radio signals at various transmitter stages. For the following reasons, at the present state-of-the-art, interfacing the optics with the radio IF section is easier than with the RF section. We avoid a baseband interface for the simple reason that radio relays are not all regenerative, that is, they are not all equipped with QAM demodulators. Therefore, it is more costly to ask for the extra regenerators needed for baseband interfacing.

Recent measurements on the error probability performance versus received optical power over the subsystems of an atmospheric optical link (including a 1.3 micron ORTEL laser, a f/11 CELESTRON C-90 transmit telescope, a similar receive telescope and a 25 GHz wide photodiode) that carried a 90 Mbps/64-QAM radio signal over a short-span laboratory test bench indicate that

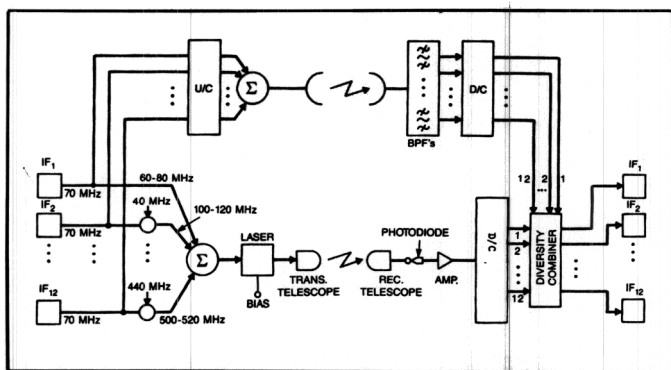


Figure 1: Proposed hybrid radio architecture

interfacing the optics with the radio in the 70 MHz IF range is easier and exhibits a better performance than its 4 GHz RF counterpart.⁶ The laser output beam was guided to the transmit telescope by an 8 micron core diameter single-mode fiber. This is to keep the optical image size in front of the telescope as small as possible in order to have a near-diffraction-limited optical geometry. On the receive side, the collected light was focused over the small active surface of a wideband photodetector. Note that the larger the demand on the electronics bandwidth is, the smaller the capacitive load of the detector has to be, hence, the smaller the active region of the photodetector has to be made. The measured average error probability versus received optical power indicates that although the laser reflection-induced intensity noise has been minimized by an optical isolator in the RF case, the IF interfacing without any countermeasure performs much better. The performance difference is attributed to the relaxation oscillation frequency of the laser being too close to the modulating signal band edge. Around its relaxation frequency, a laser is more sensitive to reflections and the spectral level of intensity noise is quite high.

In the next subsection, we will present an overview on the atmospheric optical propagation followed by a discussion of the transceiver subsystems.

Atmospheric propagation and transceiver subsystems

Atmosphere in general limits an optical transmission system performance by imposing attenuation and scattering, whether the transmitted wave is from a coherent or an incoherent source. Propagation of a coherent laser wave through turbulent atmosphere is subject to additional performance limitations. This happens because the directivity and coherence of a laser light beam, the primary reasons for the high optical system capacity, are degraded by random thermal turbulence. The thermal turbulence primarily affects the refractive index of the medium. The refractive index change, Δn , depends on physical location and time. For simplicity, the spatial and time correlation functions of Δn and their decay rates are employed in dealing with Δn .

Besides reducing the light coherence, random turbulences deflect the light beam by refraction. Beam bending changes at random with location and slowly with time such that, without some tracking means, the receiver aperture may be completely or partially missed. The coherence reduction leads to beam spreading. In both cases, the damage is a reduction of the received light intensity.

Random phase changes of the light beam in the propagation direction correspond to a lack of time coherence, that is, a random deviation in the arrival time of successive wavefronts caused by changes in the refractive index along the path, giving rise to a random frequency modulation imposed on the received signal. Random phase changes in a direction perpendicular to the propagation direction degrade the spatial coherence.

Random changes in the beam cross section due to particles and objects correspond to rapid changes in the light intensity (scintillation). The latter sets a lower limit on the modulation depth m , that is, how shallow a signal can intensity modulate the light.

To this date, no atmospheric mathematical model incorporates the impacts of fog, haze, heavy rain and snow on the transmitted light beam. Such a model would highly depend on the time and the physical location of the transmission.

Ground fog is a great source of light intensity attenuation, producing losses in the order of 0.1 dB per foot of the path length.¹ Reliable transmission under such a severe condition is extremely difficult over a long path.

The physical processes responsible for loss in the received light intensity and its lack of coherence exist even under clear weather. Briefly speaking, there are

- Refraction-induced beam deflection (beam bending);
- coherence loss giving rise to beam spread and random phase changes imposed on the light beam causing a random frequency modulation, a lack of spatial coherence, and polarization fluctuations;
- scintillation due to random changes in the beam cross-section.

The beam bending varies very slowly with time and mostly in a vertical direction. Using a simple tracking algorithm, it can be overcome.

To combat beam spreading, as a start, we must design the geometry of the optics transmission subsystems correctly in order to avoid unnecessary losses, especially in the long-haul applications where power loss can not be easily compensated for. A single-mode fiber or a sufficiently small light source is needed at the source to achieve a near diffraction-limited performance. Diffraction sets a fundamental limit on the performance of the optical system. This is due to the fact that one cannot perfectly collimate an optical beam with a finite size lens or a mirror. The minimum divergence of a

perfectly spatially-coherent source is defined by the ratio of the optical wavelength to the diameter of the radiating lens or mirror. Using this ratio, one may easily calculate the minimum loss to the geometry of the optical system at a distance, given the size of the receiver aperture.

Atmospheric causes will only add to the beam spreading, dictated by the geometry of the transmit optical subsystems. Analysis of Reference 7 shows that a Gaussian beam profile expands into a Gaussian beam with a diameter varying as the path length in kilometer to a power 1.5.

Scintillation can introduce serious problems in the transmission of QAM signals over the atmosphere. This is due to the amplitude modulation embedded in the transmitted QAM signal levels. Deleterious effects of scintillation may be reduced by increasing the modulation depth and transmitting enough average power out of the light source. If the transmit power is not enough, momentary decreases in signal-to-noise ratio causes bursts of errors in the received bitstream in digital transmission.⁸ The error bursts can be corrected using burst error correcting codes.

Selecting the wavelength of the optical beam is another very important issue to consider. Figure 7-3 of Reference 9 shows the relatively high transmissive regions called atmospheric windows. Outside these regions, the absorption and scattering of atmosphere are severely high. Unfortunately, most of the optical devices developed today aim at fiber optics transmission and a rather popular wavelength is 1.3 micron around which the atmospheric absorption is very high. Much better atmospheric windows exist around 800 and 1500 mm wavelengths.

On the receiver side, for long-haul applications, the photodetector has to be followed by a low-noise amplifier circuit. An avalanche photodetector is a good choice in this case. Various types of receiver front-ends have been described in Reference 10. Basically, the front-end types are:

- a low-impedance circuit that consists of a photodiode feeding the signal to a low-impedance amplifier. Because of the small load resistance, R_L , and the low input capacitance, C , the input time constant does not limit the front-end bandwidth;
- a high-impedance circuit in which R_L is made large to improve the receiver sensitivity; however, due to a larger time constant, the front-end is band-limited. Usually, this type of front-end has to be followed by an equalizer circuit;
- a transimpedance front-end, in which the load resistor is substituted by a large feedback resistor, and a negative-feedback around a wideband amplifier provides an increased bandwidth.

When a highly-sensitive receiver design is desired, a high-impedance front-end seems to be the best choice as suggested in Reference 10. For the hybrid radio, if an RF interface is adopted, a yet better choice is to design a tuned cavity front-end. The microwave signal bandwidth is very small compared to the radio carrier frequency. Hence, a low-noise high-Q cavity front-end can select the desired RF channel for subsequent amplifications. In any event, whether we employ an RF or an IF interface, the net effect of the low-noise amplifier is a gain G_A that helps the signal detection. In the following section we will further elaborate on this issue.

Performance analysis

We now turn our attention to intensity modulating a laser directly with an RF or an IF M-level QAM signal. The optical signal instantaneous power after intensity modulation is expressed as

$$P_T(t) = \bar{P}_T [1 + m \cdot S(t)] \quad (1)$$

where \bar{P}_T is the average transmitted light power. The modulation

index, m , is defined as

$$m = \frac{P_{\max} - \bar{P}_T}{\bar{P}_T} \quad (2)$$

where P_{\max} is the peak transmitted light power, and $S(t)$ is the M-QAM modulating signal, characterized as

$$S(t) = r_i \cos(\omega_c t + \phi_i), \quad i = 1, 2, \dots, M \quad (3)$$

where r_i and ϕ_i are random variables representing the signal amplitude and phase levels, respectively. The carrier frequency ω_c corresponds to either 70 MHz intermediate or the radio carrier frequency.

The photodetector output current corresponding to the transmitted signal is

$$I_s(t) = \rho \bar{P}_T G_o m r_i \cos(\omega_c t + \phi_i) \quad (4)$$

where ρ is the responsivity of the photodetector in Amperes/Watt or the current produced per unit optical power incident, and is defined as $\rho = \frac{e}{h\nu} \eta$, where $\left(\frac{h\nu}{e}\right)$ is the photon energy and η is the diode quantum efficiency. Parameter G_o in Equation (4) is the optical path attenuation. It is the ratio of the minimum required received power, \bar{P}_R , to meet a certain average error probability to the average transmitted power, \bar{P}_T . The mean-squared received signal component is

$$\bar{I}_s^2 = \frac{1}{2} \rho^2 m^2 \bar{P}_T^2 G_o^2 r_i^2 \quad (5)$$

The mean-squared noise portion of the photodetector current can be expressed as

$$\bar{I}_n^2 = 4kTB \frac{1}{R_L} + 2e \bar{I}_s B + \sigma_p^2 \quad (6)$$

where the first term corresponds to the mean-squared thermal current, the second term is the mean-squared shot noise current and the last term corresponds to the mean-squared reflection-induced and laser intensity-noise. In Equation (6), k corresponds to the Boltzmann's constant (1.38×10^{-23} Joules/° Kelvin), T is the absolute temperature (290° Kelvin), B is the double-sided passband signal bandwidth, e is an electron charge (1.6×10^{-19} Coul.) and \bar{I}_s is the mean received signal current that is

$$\bar{I}_s = \rho \bar{P}_T G_o \quad (7)$$

Since, the intensity noise effects are minimized through an optical isolator, one may consider the first two terms in Equation (6) as the dominant noise components. In IF interfacing of the radio with optics, the intensity noise effect is even less important. Therefore, in the following analysis we will only take the two dominant terms into account in signal-to-noise ratio evaluations.

Recall the receiver front-end amplifier gain, G_A , from the previous section. Assume an equalizer filter compensates for the frequency response in the passband.¹⁰ The value of the load resistor that minimizes the resulting mean-squared thermal current is $1/(C\omega_c)$, where C is the effective capacitance (in the order of a few pf) and ω_c is the center frequency of the passband received signal component. The minimum mean-squared thermal current is $8kTB(C\omega_c)$. Based on these assumptions, the signal-to-noise ratio (SNR) in the passband, conditioned on a given M-QAM amplitude level r_i , becomes

$$SNR | r_i = (SNR)_p r_i^2 \quad (8-a)$$

where

$$(SNR)_p = \frac{0.5 \rho^2 m^2 \bar{P}_T^2 G_0^2}{\left[\frac{8kT}{R_L G_A} + 2e(\rho \bar{P}_T G_0) \right] B} \quad (8-b)$$

We assume a symmetrical constellation for the transmitted signal, where the maximum amplitude belongs to the corner points and there is a spacing d between the points in both vertical and horizontal directions. In the absence of fading or, in general, any turbulent weather condition, the unfaded received SNR on the optical channel, after pre-detection and pre-amplification as shown in Reference 11 becomes

$$SNR_{UF} = \frac{(M - 1)}{4} \frac{\rho^2 \cdot (m^2 d^2) \cdot \bar{P}_T^2 G_0^2}{\left[\frac{8kT}{R_L G_A} + 2e\rho \bar{P}_T G_0 \right] B} \quad (9)$$

where M represents the total number of QAM levels, ρ is the responsivity of the photodiode, $m^2 d^2$ is the normalized modulation index which at most can be 0.65 (see Reference 11), R_L and G_A are the resistive load and the gain of the receiver front-end and B is the IF bandwidth of the signal. In Equation (9), G_0 is a constant path loss due to the optical subsystems' losses and beam spreading. To meet an SNR objective of 63 dB, for example, we choose $\rho = 0.7$, $m = 0.65$, $G_A = 10$ dB and a $\bar{P}_T = 100$ mw. This choice will result in a fixed path loss of $G_0 = -30$ dB which is an acceptable figure for the loss due to beam spreading and optical subsystems' losses over a typical 23-mile path. Of course, there are longer microwave hops which need an improved power budget.

A simple block diagram of a two-channel hybrid radio is depicted in Figure 2. On the optical channel, the photodetected signal contains shot-noise and receiver front-end amplifier thermal noise. Turbulent atmosphere further reduces the received light intensity. As stated in the introduction, the intensity of an optical beam propagating through a turbulent atmosphere has been characterized by a lognormal random variable whose standard deviation in decibels may extend to 25 dB in a strong turbulence.⁵ We present the actual SNR received on the optical channel as

$$\Delta_1 = 10 \log_{10} (SNR_{UF}) + 10 \log_{10}(a_o^2) \quad (10)$$

The first term in Equation (10) is fixed and the second term is the path attenuation factor which is a zero-mean Gaussian variable whose standard deviation from Reference 5, after normalization, may extend to 25 dB. Note that in Equation (10) we have essentially ignored the effect of a_o^2 on the denominator of Equation (9) by separating out the attenuation factor. Indeed, in doing so we take a penalty in SNR due to keeping the shot noise power fixed and not allowing it to reduce by the light intensity attenuation factor a_o^2 through the atmosphere. This assumption greatly simplifies the analysis, however, it makes the results somewhat conservative.

In Figure 3 we have plotted the logarithm of the probability that the light intensity attenuation level exceeds the dB levels shown on

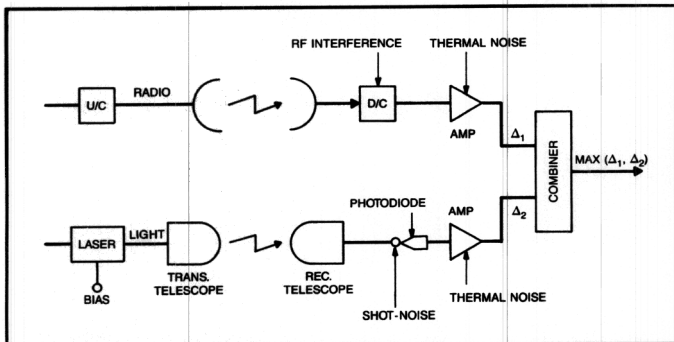


Figure 2: Microwave and optical paths schematic.

the abscissa. The different curves correspond to different values of the standard deviation of the lognormal variable. As it can be observed in the figure, intensity attenuations in the range of 50 to 70 dB are likely to occur in a strong turbulence condition when the lognormal variable has a standard deviation of 22 dB.

The radio channels need be operational when the optical channel is down due to weather related problems. As stated in the introduction, during such times the former should only be subject to small-variance flat fades³ and perhaps larger flat fades with a shallow notch superimposed on them. To incorporate the latter type of fades, we can safely extend the standard deviation of the flat energy loss, which is assumed to be lognormal, to 7 dB. This, as shown in Figure 4, makes flat fades of up to 20 dB level likely to occur on the radio channel. This figure is similar to Figure 3 in structure and demonstrates the likelihood of radio channel flat fade levels for various values of standard deviation of the lognormal fading parameter.

The radio signal also suffers from RF interference as received. Conditioning on the interference amplitude level and using the fact that noise and interference are independent, the signal-to-noise-plus-interference ratio at the IF stage can be expressed as

$$SNIR | I = \frac{SIR \cdot \gamma_o}{SIR + \gamma_o} \cdot a_r^2 \quad (11)$$

where in Equation (11), the left-hand side denotes the signal-to-in-

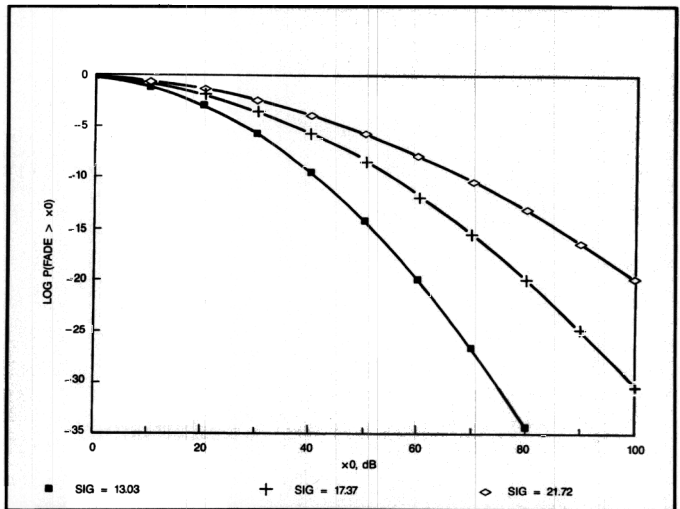


Figure 3: Optics channel fading.

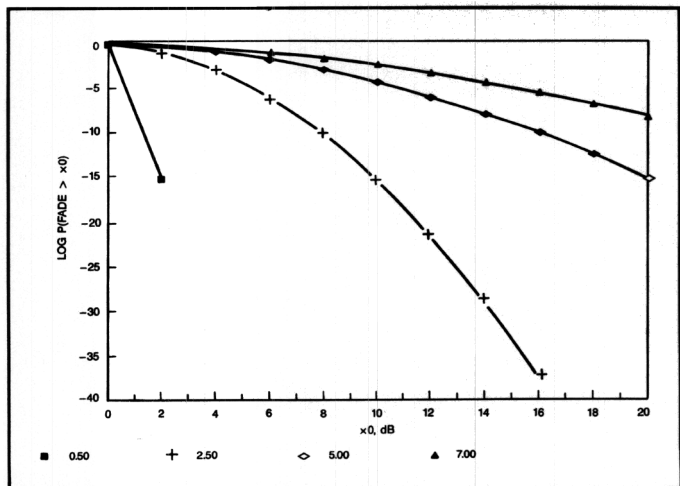


Figure 4: Radio channel fading.

interference-plus-noise ratio conditioned on the interference level, SIR is the signal-to-interference power ratio, γ_o is the unfaded SNR received at the receiver IF and α_r^2 is the lognormal flat fade level on the radio channel.

Again, in dB's we denote $(SNIR | I)$ by $(\Delta_2 | I)$, expressed as

$$\Delta_2 | I = 10 \log_{10}(SNIR | I) + 10 \log \alpha_r^2 \quad (12)$$

where in Equation (12), the first term is a constant and the second term is a zero-mean Gaussian variable with a standard deviation of less than or equal to 7 dB. The unfaded SNR, γ_o , in Equation (11) is assumed to be 63 dB as we assumed for the optical channel.

Now, in the absence of a deep frequency-selective fade notch on the radio signal, "the hybrid radio promise", a selection diversity combiner at IF or RF can select the channel that receives the maximum signal-to-total noise power ratio, as stated in the introduction. Since the received SNR on the optical channel and the conditional signal-to-noise plus interference power ratio on the radio channel are both Gaussian random variables, the probability density of the maximum of the two is indeed the power signal-to-noise ratio probability density at the combiner output.

Recall that we chose the maximum (unfaded) signal-to-noise ratio on each channel to be 63 dB. For the combiner output signal-to-noise ratio to be 63 dB, at least one of the two SNR's has to be 63 dB and the other can vary anywhere between 0 and 63 dB. Hence, mathematically the cumulative distribution function (CDF) of the combiner output SNR, Δ , corresponds to the product of the CDF of the SNR's on the input channels.¹² For the two Gaussian variables we can express this as

$$F_{\Delta|I}(\delta) = \left[-\frac{1}{2} \operatorname{erfc}\left(\frac{\delta - m_{\Delta_1}}{\sqrt{2} \sigma_{\Delta_1}}\right) \right]$$

$$\cdot \left[1 - \frac{1}{2} \operatorname{erfc}\left(\frac{\delta - m_{\Delta_2|I}}{\sqrt{2} \sigma_{\Delta_2|I}}\right) \right] \quad (13)$$

where m_{Δ} and σ_{Δ} refer to mean and standard deviation of the output SNR, δ is the random variable, and,

$$\operatorname{erfc}(x) = \frac{2}{\sqrt{\pi}} \int_x^{\infty} e^{-t^2} dt.$$

Using Equation (13), we can determine the probability density function (pdf) of $\Delta | I$, that is the pdf of the conditional SNR at the combiner output as

$$\begin{aligned} f_{\Delta|I}(\delta) = & \frac{1}{\sigma_{\Delta_2|I} \sqrt{2\pi}} \exp\left[-\frac{(\delta - m_{\Delta_2|I})^2}{2\sigma_{\Delta_2|I}^2}\right] \\ & \left[1 - \frac{1}{2} \operatorname{erfc}\left(\frac{\delta - m_{\Delta_1}}{\sqrt{2} \sigma_{\Delta_1}}\right) \right] \\ & + \frac{1}{\sigma_{\Delta_1} \sqrt{2\pi}} \exp\left[-\frac{(\delta - m_{\Delta_1})^2}{2\sigma_{\Delta_1}^2}\right] \\ & \left[1 - \frac{1}{2} \operatorname{erfc}\left(\frac{\delta - m_{\Delta_2|I}}{\sqrt{2} \sigma_{\Delta_2|I}}\right) \right] \end{aligned} \quad (14)$$

The conditional outage is simply the area under the pdf over a range of combiner output SNR for which the objective average bit error probability cannot be met.

$$\text{outage} | I = \int_0^{\Delta_0} f_{\Delta|I}(\delta) d\delta \quad (15)$$

where Δ_0 is the threshold value of SNR at the combiner output below which the bit error rate (BER) objective is not met.

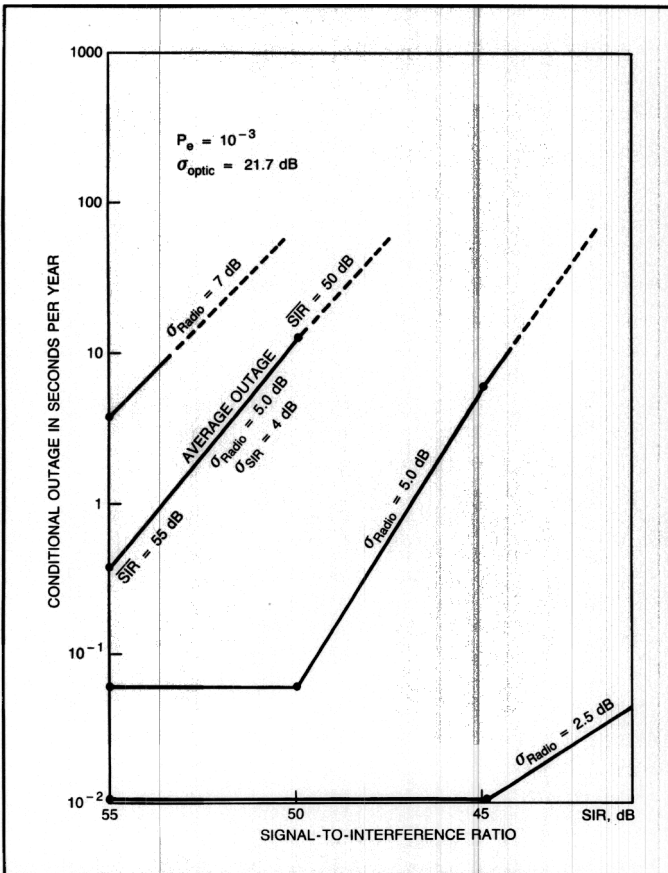


Figure 5: Conditional outage in seconds per year versus fixed value SIR, dB.

In Figure 5 we have plotted the conditional outage in second per year versus different values of SIR in dB. The curves have been plotted to correspond to different values of standard deviation of the fading parameter (the lognormal variable) of the microwave channel. The values range from 2.5 dB to 7 dB. All these curves have been plotted for an optical channel intensity attenuation standard deviation of 22 dB. The threshold objective error probability is assumed to be 10^{-3} . That is, the system is considered in outage when the threshold bit error rate (BER) is exceeded. The second and third curve from the top on this figure correspond to average outage and conditional outage, respectively. As observed, once the statistics of the interference is incorporated, the actual outage (curve 2) is worse than the conditional counterpart (curve 3). We will elaborate on this point later in this section. It is seen that for the most part, the conditional outage is less than 10 seconds per year, the standard outage objective.

Measurements in Reference 4 reveal that the amplitude of the interference, for the most part, follows a lognormal probability density and in decibels, the mean SIR is close to 60 dB and the standard deviation of SIR is about 4 dB. The pdf of interference amplitude is expressed as

$$f_I(i) = \frac{1}{i \sigma_x \sqrt{2\pi}} \exp\left\{-\frac{[\ln(i) - \overline{\ln(i)}]^2}{2\sigma_x^2}\right\}$$

where $x = \ln(i)$ is Gaussian with mean $\overline{\ln(i)}$ and standard deviation σ_x .

Using the pdf of $\Delta | I$, we can remove the conditioning by integrating the pdf over the pdf of the interference. The

$$\overline{\text{outage}} = \int_I (\text{outage} | I) f_I(i) di. \quad (17)$$

σ Radio, dB \ σ Optic, dB	0.5	2.5	5.0	7.0
13.0	0	2×10^{-8}	2×10^{-3}	9.5×10^{-2}
17.4	0	2×10^{-7}	2×10^{-2}	9.5×10^{-1}
21.7	0	7×10^{-7}	6×10^{-2}	3

σ Radio, dB \ σ Optic, dB	0.5	2.5	5.0	7.0
13.0	0	4×10^{-5}	4×10^{-2}	5.3
17.4	0	2×10^{-4}	2×10^{-1}	32.6
21.7	0	6×10^{-4}	6×10^{-1}	79.2

The average outage obtained this way can be estimated numerically for various channel conditions.

Tables 1 and 2 illustrate the average outage in seconds per year for the threshold objective BER values of 10^{-3} and 10^{-9} , respectively, for various fading conditions on the optical and microwave channels. The fading parameter in these tables is the standard deviation of lognormal attenuation factors on the two channels. Referring with the values specified in the tables to Figures 3 and 4, we can see for example, a 21.72 dB standard deviation for the intensity attenuation factor on the optical channel from Figure 3 corresponds to an attenuation level between 20 to 30 dB occurring with a rather high probability. The average outage values in the tables were obtained using the statistics of the interference, as stated earlier. As observed in Table 1, for a threshold objective BER = 10^{-3} , the maximum outage is 3 seconds/year. In Figure 6, we have plotted the average outage in seconds/year versus various values of mean SIR for the worst-case fades of both microwave and optical channels. Again, a threshold objective BER = 10^{-3} is desired. The SIR standard deviation is kept at 4 dB. As observed, down to an average SIR of 57 dB, the 10 seconds/year average outage objective is met.

In general, incorporating the statistics of the interference into outage estimates results in larger outage estimates compared to when a fixed SIR is employed in calculations.

Conclusions

In this paper, we presented a hybrid radio model that uses frequency-division-multiplexed radio IF's to intensity modulate a laser and to provide a parallel optical diversity link for all the radio channels. Using the assumption of negative-correlation between dispersive fading of the radio and fading on the optical channel, we developed a simple performance assessment model. Performance results in the form of outage in seconds per year were presented for various optical and radio channel conditions. The optical diversity channel provides sufficient protection against both interference and fading of radio channels. Careful experimental study of flat and dispersive fades across the entire radio band and their correlation with fades on the optical channel can truly tell how well the proposed structure will perform. Even though the outage of the two links cannot be assumed to occur in totally different conditions, there is no doubt a diversity advantage to using this approach, and the analysis given here could form part of an overall estimate of

outage. The immunity of the optical link to interference makes the scheme worth pursuing. However, the only way to estimate the probability of simultaneous outages of both microwave and optical links due to meteorological structures that produce fog, and that the only way to estimate the outage on a typical system is to carry out an experiment.

Acknowledgment

This work was partially supported by the Telecommunications Research Institute of Ontario (TRIO), Photonic Networks and Systems Thrust.

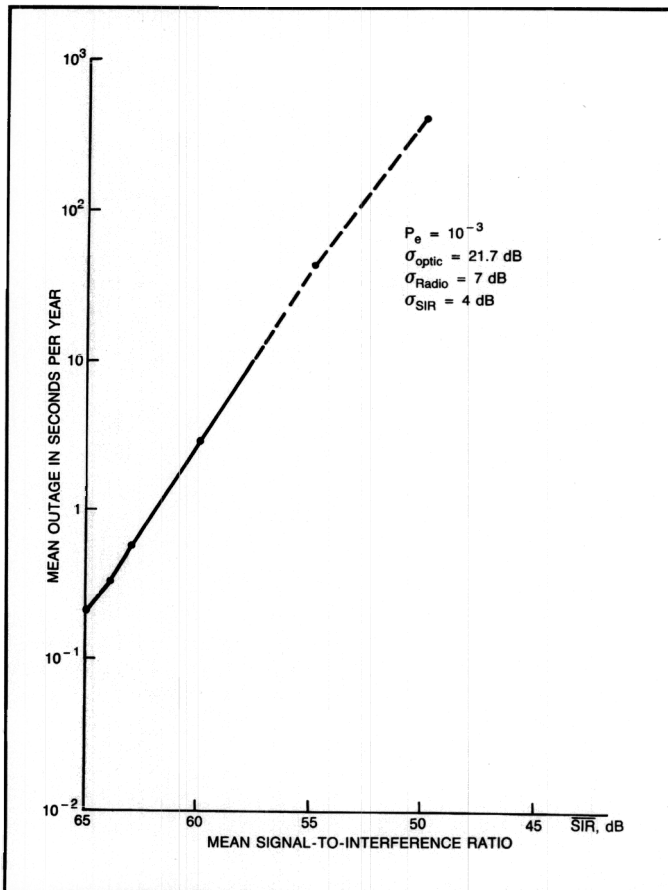


Figure 6: Mean outage in seconds per year versus mean SIR, dB.

References

- King, B.G., Fitzgerald, P.J., and Stein, H.A., "An experimental study of atmospheric optical transmission," *The Bell System Technical Journal*, Vol. 62, No. 3, March 1983.
- Owen, N., et al., "Analysis of multipath fading observations on certain microwave paths in British Columbia," *Proceedings of URSI Commission F Symposium, ESA SP-194*, European Space Agency, Paris, 1983.
- Babler, G.M., "Scintillation effects at 4 and 6 GHz on a line-of-sight microwave link," *IEEE Trans. on Antenna and Propagation*, Vol. AP-19, No. 4, July 1971.
- Adenigba, A.B., and Tsolakis, T.A., "Interference dynamics considerations in digital radio performance," *Proceedings of ICC'88*, June 1988.
- Last, I., et al., "Level crossing and fading probabilities in an atmospheric communication link for a non-Markov process," *Journal of Applied Optics*, Vol. 25, No. 7, April 1986.
- Kavehrad, M., "Unpublished work."
- Strohbehn, J.W., ed., *Laser beam propagation in the atmosphere*, Springer Verlag, 1976, chapter 5, 1978.
- Young, P.W., "Impact of temporal fluctuations of signal-to-noise ratio (burst errors) on free-space laser communications system design," *Proceedings of SPIE, Int. Soc. Opt. Eng.*, Vol. 616, 1986, pp. 174-181.
- Pratt, W.K., *Laser Communication Systems*, John Wiley & Sons, Inc., 1969, chapter 7.
- H Kressel ed., *Semiconductor Devices for Optical Communications*, Springer Verlag, 1980, chapter 4.
- Kavehrad, M., and Savov, E., "Fiber-optic transmission of microwave 64-QAM signals," *IEEE Journal on Selected Areas in Communications*, September 1990.
- Papoulis, A., *Probability, Random Variables, and Stochastic Processes*, McGraw-Hill, 1965, chapter 7.